Supporting Material

"Contractile equilibration of single cells to step changes in extracellular stiffness"
by A. Crow, K.D. Webster, *et al.*

Conversion from stiffness to elasticity

We use a simple conversion that assumes cell height is on the order of 10 μm and contact area on the order of 100 μm^2. Young's modulus can then be calculated according to

$E = \frac{kH_{cell}}{A_{contact}} = 0.1k$ (where k is in nN/μm and E is in kPa).

Calculation of model parameters for a contracting cell

The model predictions may be retroactively applied to the data to get median and percentile values for the independent actuator rate, α, and viscoelastic parameters as follows:

$$\alpha = \left(\frac{dX}{dt} \right)_{k_{ex}=0, t \gg \tau}$$

$$k_1 = \frac{\left(\frac{dF}{dt} \right)_{k_{ex}=\infty, t \gg \tau}}{\left(\frac{dX}{dt} \right)_{k_{ex}=0, t \gg \tau}}$$

$$k_2 = k_1 \left(\frac{\tau_{k_{ex}=0}}{\tau_{k_{ex}=\infty}} - 1 \right)$$

$$\gamma = k_1 \tau_{k_{ex}=\infty}$$

where τ is the response timescale. Calculations based on the median, 25th and 75th percentile values reported yield the following presented as median (25th percentile, 75th percentile):

Table S1. Model Parameters calculated based on data.

	α (nm/s)	k_1 (nN/μm)	k_2 (nN/μm)	γ (nN*s/μm)
Control	-13 (-8.3, -20)	36 (35, 37)	53 (27, 75)	140 (78, 240)
30 μM Blebbistatin	-4.8 (-3.5, -6.7)	16 (12, 23)	25 (14, 34)	89 (82, 90)
500 nM Cyto D	-6.7 (-3.8, -10)	15 (7.0, 23)	12 (3.1, 46)	64 (51, 83)
10 nM Jasplakinolide	-15 (-9.3, -24)	26 (16, 27	40 (11, 62)	89 (48, 98)
30 μM Nocodazole	-4.7 (-2.5, -6.3)	93 (73, 97)	140 (48, 190)	340 (210, 600)
25 μM pp2	-14 (-8.2, -17)	40 (34, 58)	85 (61, 110)	140 (92, 150)
30 μM FAK inhibitor	-6.7 (-3.7, -9.5)	42 (11, 53)	52 (12, 67)	170 (60, 180)
200 μM Gadolinium	-9.2 (-5.9, -16)	51 (43, 55)	110 (38, 120)	170 (92, 240)

The calculated viscoelastic parameters reveal interesting inhibition-based trends that are not visible by simply studying the response timescale. Specifically, both elastic and viscous parameters decrease for blebbistatin and cytochalasin D treated cells while elastic and viscous parameters increase for nocodazole-treated cells. These changes in mechanical properties are not observed in the response timescale because elastic and viscous properties have opposing effects: $\tau_{k_{ex}=0} = \gamma\left(\frac{1}{k_1}+\frac{1}{k_2}\right)$. Therefore corresponding increases or decreases in both parameters may cancel resulting in a response timescale consistent with the control. The decrease in elastic components in the cases of blebbistatin and cytochalasin D and the increase in elastic components in the case of nocodazole are consistent with previously published results (1). To further examine the role of actin structures, we stabilized the actin cytoskeleton with Jasplakinolide. This had a similar effect to cytochalasin D in that 10 nM Jasplakinolide had no effect on the response timescale compared to the control, but 50 nM was adequate to stop contraction altogether. Calculation of viscoelastic parameters in the presence of 10nM Jasplakinolide reveals a slight decrease in all values to yield a response timescale indistinguishable from the control, as shown in Table S1. In the case of blebbistatin, the decrease in the viscous component is not as great and therefore does not fully cancel the decrease in elastic component, resulting in a response timescale distinct from control.

Inhibition of FAK, Src family kinases, or stretch-activated ion channels did not yield any major difference in k_1 or γ components compared to the control in our system. We note that the internal spring parameter k_2 shows the greatest inhibition-induced changes compared to the control in all cases, including focal adhesion signaling. We therefore

expect we may see a difference in response timescale for extreme step increases in stiffness: $\tau_{k_{ex}=\infty} = \frac{\gamma}{k_2}$. While we do anecdotally observe the expected trends, we are unable to show statistical significance with the limited number of force trace intervals that pass our F-test criterion. We therefore leave investigation of this intriguing phenomenon to a subsequent study.

Derivation of the response of the model to step changes in stiffness

The equations for the model are:

$$f(t) = k_1(x_1 - \alpha t) + f_2$$
$$f_2 = k_2 x_2 = \gamma \dot{x}_3$$
$$x_1 = x_2 + x_3$$

where $f(t)$ is the tensile force applied at the cell-cantilever interface, α is the velocity at which the reference length of the spring x_1 is changing (i.e., this is the actuator), and x_2 and x_3 describe the state of the internal spring and dashpot, respectively.

In the experiment, the effective stiffness jumps at the set of times $\{t_j\}_{j=1}^{j=N}$. This can be described within the model by setting

$$f(t) = f(t_j) - k_{ex}(t_j)\left(x_1 - x_1(t_j)\right)$$

for $t \in \left[t_j, t_{j+1}\right)$ where $k_{ex}(t)$ is the applied stiffness at time t. When the intervals between jumps in stiffness are very long, $t \gg \tau$, we can analyze the model by considering its behavior for a single jump. First we define: $t' = t - t_j$ and

$$x_1'(t') = x_1(t' + t_j) - x_1(t_j)$$
$$x_2'(t') = x_2(t' + t_j)$$
$$x_3'(t') = x_3(t' + t_j) - x_1(t_j)$$

so that the equations take the form

$$f(t_j) - k_{ex}(t_j)x_1' = k_1(x_1' - \alpha t') + k_1(x_1(t_j) - \alpha t_j) + f_2$$
$$f_2 = k_2 x_2' = \gamma \dot{x}_3'$$
$$x_1' = x_2' + x_3'$$

This can be rearranged to

$$f' = k_1'(x_1' - \alpha' t') + f_2$$
$$f_2 = k_2 x_2' = \gamma \dot{x}_3'$$
$$x_1' = x_2' + x_3'$$

with

$$k_1' = k_1 + k_{ex}\left(t_j\right)$$

$$\alpha' = \frac{k_1}{k_1'}\alpha$$

$$f' = f\left(t_j\right) - k_1\left(x_1\left(t_j\right) - \alpha t_j\right)$$

The solution of this model is

$$x_3'\left(t'\right) = x_3'\left(0\right)\exp\left(-\frac{t'}{\tau}\right) + \frac{f'}{k_1'}\left(1-\exp\left(-\frac{t'}{\tau}\right)\right) + \alpha'\left(t' - \tau\left(1-\exp\left(-\frac{t'}{\tau}\right)\right)\right)$$

$$x_1'\left(t'\right) = \frac{f'}{k_1'} - \left(\frac{f'}{k_1'} - x_3'\left(0\right)\right)\left(\frac{k_2}{k_2+k_1'}\right)\exp\left(-\frac{t'}{\tau}\right) + \alpha'\left(t' - \tau\left(1-\exp\left(-\frac{t'}{\tau}\right)\right) + \frac{\gamma}{k_2}\left(1-\exp\left(-\frac{t'}{\tau}\right)\right)\right)$$

$$\tau = \gamma\left(\frac{1}{k_1'} + \frac{1}{k_2}\right)$$

and for long stiffness intervals we find

$$x_3'\left(t'\right) \approx \alpha' t' + \frac{f'}{k_1'} - \alpha'\tau$$

$$x_1'\left(t'\right) \approx \alpha' t' - \alpha'\tau + \frac{\gamma\alpha'}{k_2} + \frac{f'}{k_1'}$$

Using these asymptotic relations we can deduce the values of $x_3'\left(0\right)$ and f' immediately following a change in stiffness at $t = t_{j+1}$, let us call these $x_3''\left(0\right)$ and f''. Assuming $t' \gg \tau$ so that we can use the asymptotic formulas, with the recurrence formula for $f\left(t\right)$ and the formula for τ we find $f'' = \gamma\alpha'$. We can also easily find that $x_3''\left(0\right) = -\frac{\gamma}{k_2}\alpha'$.

These formulas can be used to give the final complete solution for changes in stiffness with long time intervals as

$$x_1\left(t\right) - x_1\left(t_{j+1}\right) = \alpha\frac{k_1}{k_1 + k_{ex}\left(t_{j+1}\right)}\left(t - t_{j+1}\right)$$
$$+\alpha\frac{k_1\gamma}{k_1 + k_{ex}\left(t_{j+1}\right)}\left(\frac{1}{k_1 + k_{ex}\left(t_j\right)} - \frac{k_1}{k_1 + k_{ex}\left(t_{j+1}\right)}\right)\left(1-\exp\left(-\frac{t - t_{j+1}}{\tau_{j+1}}\right)\right)$$

where

$$\tau_{j+1} = \gamma\left(\frac{1}{k_1 + k_{ex}\left(t_{j+1}\right)} + \frac{1}{k_2}\right)$$

The increment to the measured force during the interval $\left[t_{j+1}, t_{j+2}\right)$ can be derived from this relation by multiplying by $k_{ex}\left(t_{j+1}\right)$, and in the case of a displacement clamp, taking the limit $k_{ex}\left(t_{j+1}\right) \to \infty$.

References

1. Sen, S., and S. Kumar. 2009. Cell-Matrix De-Adhesion Dynamics Reflect Contractile Mechanics. Cellular and molecular bioengineering. 2: 218-230.

Supporting Figures

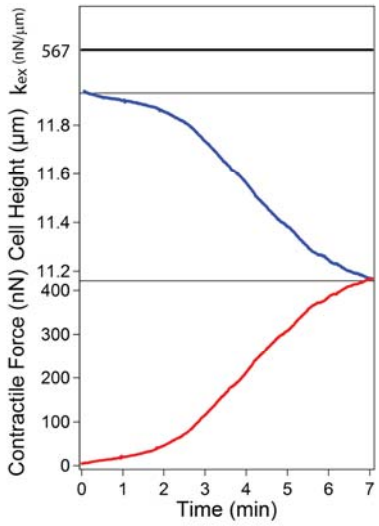

Fig. S1. Contractile behavior of single cell under constant stiffness. Under a constant extracellular stiffness, k_{ex}, here presented as the stiffness of the cantilever, the cell originally accelerates (decreasing cell height and increasing contractile force) to a constant contraction velocity and traction rate. This linear regime is maintained over several minutes before slowing. We consistently observe this linear contractile regime whereas behavior upon slowing is variable ranging from a temporary tensional equilibrium at constant force to the cell releasing one surface resulting in a decrease in contractile force and lengthening of the cell. Note a stable steady-state force/height is never permanently reached in our setup due to the motile nature of fibroblasts. All stiffness response data were collected from the middle linear regime of contraction.

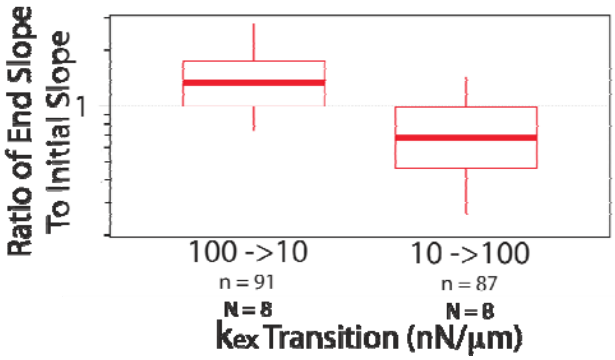

Fig. S2. Same trend observed for force trace as for height trace upon a step change in stiffness. The ratio of the slope over the last quarter of the interval to the slope over the first quarter of the interval is calculated for each 20-second stiffness interval for the force trace. At a given stiffness, the force and height traces are directly related by the extracellular stiffness. Therefore by definition of the system we observe the same trend as seen for the height trace in Figure 2g. n represents number of stiffness transitions, N represents number of cells, and box plot presents median, 25th and 75th percentile and 10 and 90th percentile outliers.

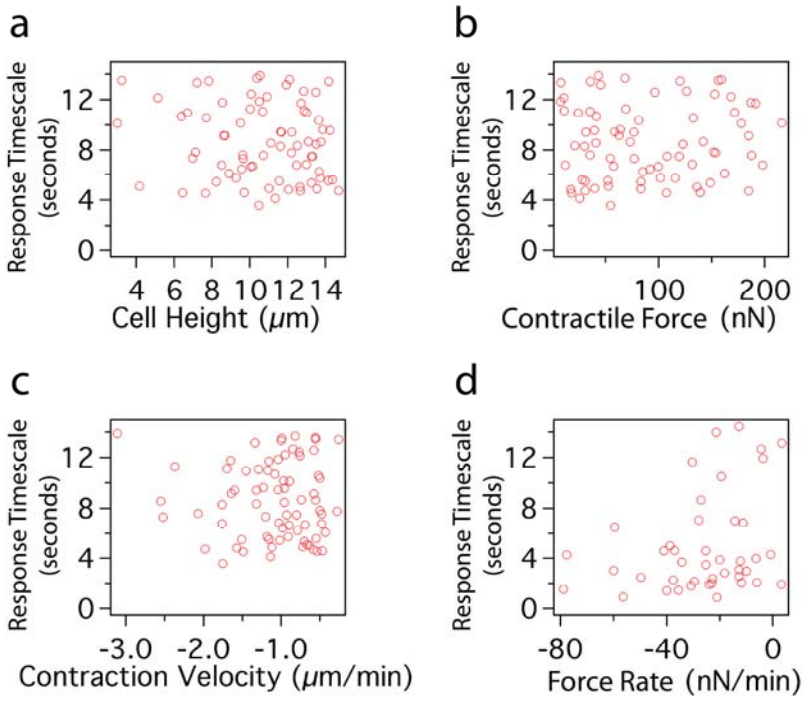

Fig. S3. Response timescale is independent of contractile force, cell height, force rate, and contraction velocity. Response time was not statistically significantly correlated with (a) cell height, (b) contractile force, (c) contraction velocity, (d) or force rate, as determined by Spearman's rank correlation analysis ($p>0.2$).

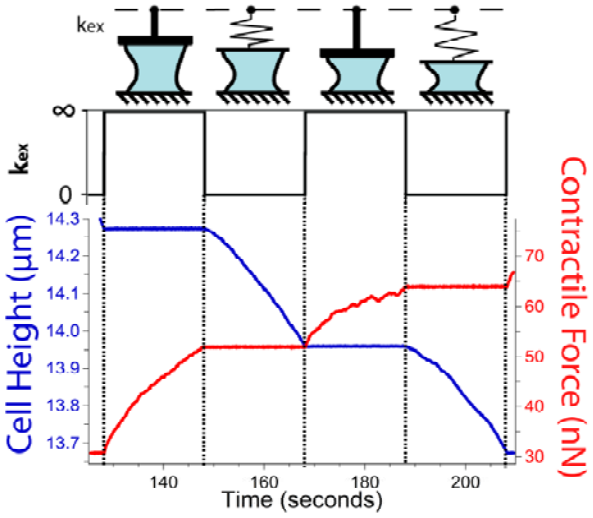

Fig. S4. Contractile response of a cell to changes in stiffness in the presence of 30 μM blebbistatin. At an intermediate dose of blebbistatin, acto-myosin contraction is slowed, but the seconds timescale acceleration upon a reduction in stiffness and deceleration upon an increase in stiffness are present. However, the median response timescale is 52% longer with 30 μM blebbistatin than for the control.

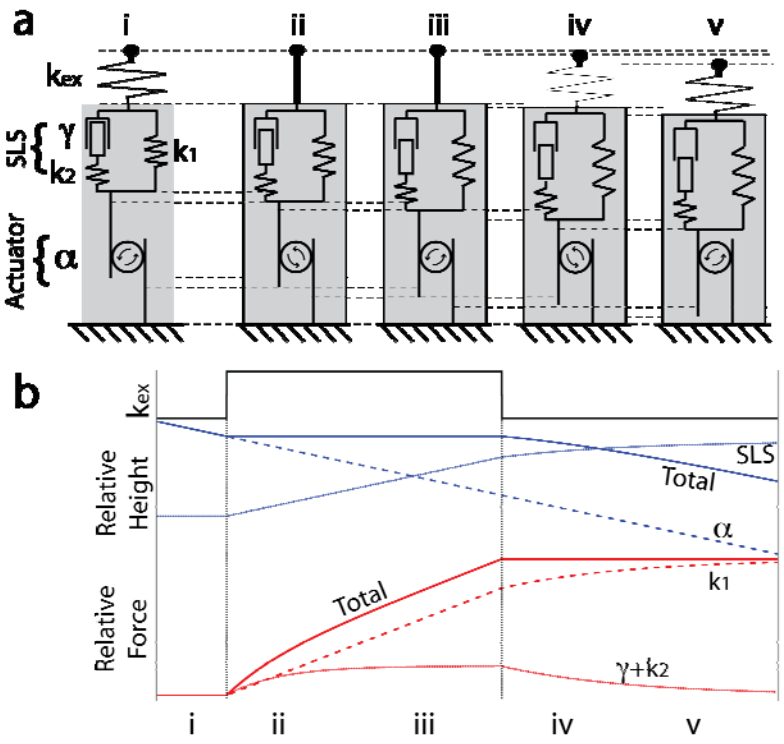

Fig. S5. Detailed explanation of mechanical model. (a) Cartoon illustrating the independent actuator moving at rate α in series with the standard linear solid (SLS) element consisting of a spring k_2 and dashpot γ in parallel with a spring k_1. As extracellular stiffness conditions change, different elements of the SLS absorb the sudden change in stiffness as illustrated. (b) Predictions of the model perfectly simulate the observed response for a step increase and step decrease in stiffness, for both the height and force behavior, as shown by the solid lines labeled "Total" (indicating whole-cell behavior). The activity of individual elements is indicated by dashed lines. For the height trace, the change in height of the actuator is constant as indicated by the linearity of the trace marked α. The standard linear solid element (SLS), however, equilibrates to the step change in extracellular stiffness. For the force channel, the individual activity of the two sides of the SLS model are shown: the lone spring k_1 and the spring and dashpot in series: k_2+γ. The sum of these two curves yields the total force exerted by the whole-cell. The roman numerals indicate corresponding time points in (a) and (b).